Fast Parameters Extraction of General Three-Dimension Interconnects Using Geometry Independent Measured Equation of Invariance

Weikai Sun   Wayne Wei-Ming Dai   Wei Hong

Board of Studies in Computer Engineering
University of California, Santa Cruz, CA 95064

Dept. of Radio Eng.
Southeast Uni., Nanjing, PRC

Abstract

Measured Equation of Invariance(MEI) is a new concept in computational electromagnetics. It has been demonstrated that the MEI technique can be used to terminate the meshes very close to the object boundary and still strictly preserves the sparsity of the FD equations. Therefore, the final system matrix encountered by MEI is a sparse matrix with size similar to that of integral equation methods. However, complicated Green's function and disagreeable Sommerfeld integrals make the traditional MEI very difficult, if not impossible, to be applied to analyze multilayer and multiconductor interconnects. In this paper, we propose the Geometry Independent MEI(GIMEI) which substantially improved the original MEI method. We use GIMEI for capacitance extraction of general three-dimension VLSI interconnect. Numerical results are in good agreement with published data and those obtained by using FASTCAP [1], while GIMEI is generally an order of magnitude faster than FASTCAP and uses significant less memory than FASTCAP.

1 Introduction

Analysis and design of interconnections in high speed VLSI chips, multichip models (MCM), printed circuit boards (PCB) and backplanes are gaining importance due to the rapid increase in operating frequencies (with the rise time of digital signals dropping into subnanosecond range) and decrease in feature sizes (with deep submicron process technology). Actually now, the interconnect delay has dominated the total path delay. Therefore, it is necessary to develop computationally efficient methods to extract the parasitics of the interconnects. For an inhomogeneous structure like VLSI interconnects, the modes are hybrid and full-wave approach should be adopted. However, the qausi-static(qausi-TEM) approximations are sufficiently accurate when the transverse components predominates over the longitudinal ones, in other words, the transverse dimensions of the structure are much smaller than wavelength, which is just the case in the interconnects we are concerning about. Therefore, in this paper, we adopt the quasi-TEM assumption. In fact, up to now the static capacitance matrix $[C]$ and inductance matrix $[L]$ of the multilayer and multiconductor interconnect is commonly used in practice for high-speed VLSI, PCB and MCM design.

The various procedures to get the solution can be generally classified into two categories. One category is to solve differential Maxwell equations called domain methods, such as Finite Element Method(FEM) [2] and Finite Difference Method(FDM) [3]. They basically divide the space surrounding the object into meshes, then write local equations at each mesh point, which leads to a sparse matrix system. But the standard FD(or FE) method involves large number of unknowns because they get the solution of the potential distribution over the entire geometry domain and the boundary conditions are valid only at the space far away from the object. The other category is using the integral equation approach such as Method of Moments(MoM) [4], Boundary Element Method(BEM) [5], and BEM with multipole acceleration [1]. They make meshes on the surface of the object. Compared to FD, this greatly reduces the number of unknowns. But each small piece is either source or field point, and affected by all others, which leads to a full matrix. Therefore, the existing methods either solve a sparse but very large matrix or a small but full matrix.

Measured Equation of Invariance(MEI) is a new concept in computational electromagnetics [6, 7, 8, 9]. MEI is used to derive the local finite difference (FD) like equation at mesh boundary where the conventional FD approach fails. It is demonstrated that the MEI technique can be used to terminate the meshes very close to the object boundary and still strictly preserves the sparsity of the FD equations. Therefore, the final system matrix encountered by MEI is a sparse matrix with size similar to that of integral equation methods, which results in dramatic savings in computing time and memory usage compared to other known methods. It has been successfully used to analyze electromagnetic scattering problems and microwave integrated circuits. For multilayer and multiconductor struc-

33rd Design Automation Conference ®

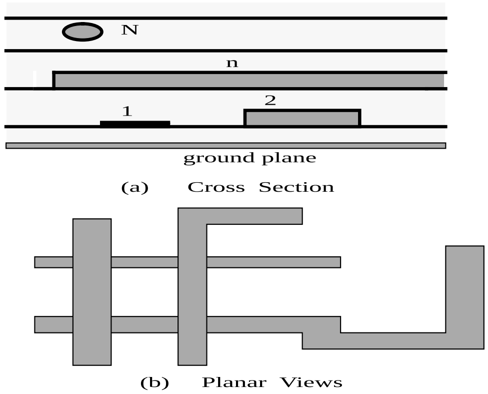

Figure 1: A general 3D interconnect configuration, the two figures are not related

tures, however, the deduction of Green's function is very difficult. Also the calculation of the MEI coefficients will encounter many Sommerfeld type integrals. As the result, the calculation of MEI coefficients dominates the total computing time. Therefore, complicated Green's function and disagreeable Sommerfeld integrals make the traditional MEI very difficult, if not impossible, to be applied to analyze multilayer and multiconductor interconnects.

Recently, a MEI variety called Geometry Independent MEI(GIMEI) was proposed [10] which was verified to be extremely computationally efficient, and has been successfully used to solve two-dimension VLSI interconnect problems. Geometry Independent MEI substantially improved the MEI in three key aspects: 1) cancelled the postulate of geometry specific in conventional MEI, 2) avoided the deduction of Green's function in multilayer structure, and 3) avoided the calculation of disagreeable Sommerfeld type integrals. Using this method, the calculation of MEI coefficients represents small percentage of the total computing time. In this paper, we extended Geometry Independent MEI to compute capacitance matrix of general three-dimension interconnects. The results are in good agreement with published data and those obtained by using FASTCAP [1]. GIMEI is generally an order of magnitude faster than FASTCAP and uses significantly less memory than FASTCAP.

2 Problem Formulation

A general interconnect configuration is shown in Fig. 1. For an N-conductor system, an $N \times N$ capacitance matrix is defined by $Q_i = C_{ii}\Phi_i + \sum_{j=1}^{N} C_{ij}(\Phi_i - \Phi_j)$, which can be rewritten as: $Q_i = \sum_{j=1}^{N} C_{ij}^s \Phi_j$, where Q_i and Φ_i are total charge and potential on ith conductor respectively, and C_{ij}^s is the short circuit capacitance. We have the transformation: $C_{ii} = \sum_{j=1}^{N} C_{ij}^s$, and $C_{ij} = -C_{ij}^s$ for $i \neq j$. In the remaining of the paper, when talking about capacitance, we refer to the short circuit capacitance. Now, the problem of computing parasitic capacitance is reduced to the problem of calculating the charge on each conductor for known potentials.

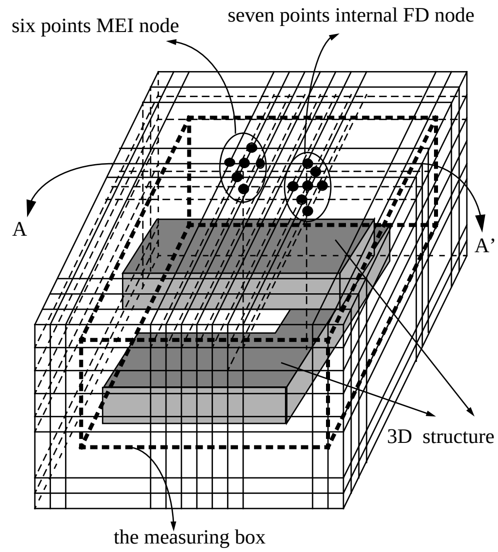

Figure 2: Discretization mesh of 3D structure

We first discretize the geometry of interest into elementary boxes using a three dimensional Cartesian grid as shown in Fig.2. The electrical potential can be assumed to be constant inside the elementary boxes and confined at the middle of the box. The mesh points on the metalization can be treated to be at a constant potential under the qausi-TEM assumption. The boundary of the mesh is treated later when we present the concept of MEI.

The electrical potential function ϕ in the bounded region except those mesh points on conductors with the quasi-static assumption satisfies the following Laplace equation:

$$\frac{\partial^2 \phi}{\partial x^2} + \frac{\partial^2 \phi}{\partial y^2} + \frac{\partial^2 \phi}{\partial z^2} = 0 \qquad (1)$$

Using difference to approximate derivative, we can write the electric potential at each internal mesh point as the linear combination of potentials of neighboring mesh points. We have also developed general local FD equations for the conventional seven points FD net, which can handle non-uniformly distributed structures and materials. And it can be proven that the local FD equations have the error of the order of $O(h^2)$, where $h = max(h_x, h_y, h_z)$. By using loop integral technique, we can also easily obtain the local FD equations with all six different discretization distances.

3 Measured Equation of Invariance

The above derived FD equation is only applicable at interior nodes of the mesh. K.K. Mei postulated [6] that the finite difference/element equations at the mesh boundary points may be represented by a local linear equation of the type

$$\sum_{i=0}^{M} C_i \phi_i = 0 \qquad (2)$$

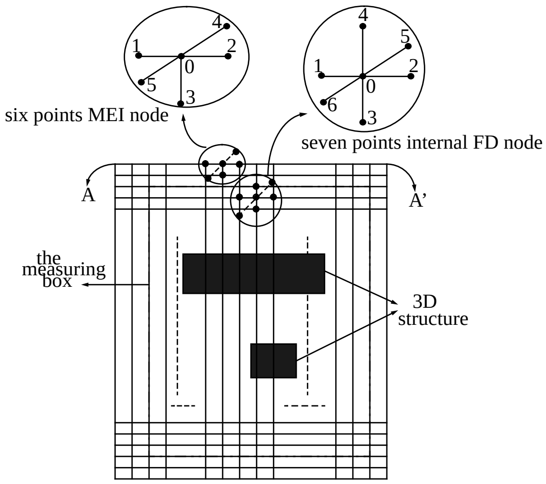

Figure 3: A slice from Fig.2 illustrating measuring box

where M is the number of nodes that surrounding the node of interest ϕ_0. The node configuration is shown in Fig. 3 which is a cross section of the cube shown in Fig.2 with the surfaces A and $A^{'}$. The coefficients in Eq.2 are: (i) location dependent, (ii) geometric specific, (iii) invariant to the excitation. Eq. 2 is called measured equation of invariance (MEI), and C_i, $i = 0, \ldots, M$, the coefficients of MEI. In conventional MEI, distribution functions, called "metrons", are excited on the conductors and the potential values on the MEI nodes as shown in Fig. 2 and Fig. 3 are obtained from the integrals of the metrons multiplied by Green's function. Substituting the potential values at MEI nodes into MEI (Eq. 2) leads to a set of linear algebraic equations with respect to the MEI coefficients $C_i(i = 1, \ldots, M)$, where each equation corresponding to one metron. The MEI coefficients are determined by solving the linear algebraic equations. Finally, the potential values at all nodes can be obtained by solving the system of linear algebraic equations which consist of FD equations at interior nodes and MEI at truncated mesh boundary nodes. The coefficient matrix is a sparse matrix since each row contains either seven non-zero elements from FD equations or M(at most six) non-zero elements from MEI. It results in great savings in the memory needs as compared with MoM and BEM. Furthermore, the computing time is proportional to N^2 for solving a sparse matrix equation but N^3 for solving a full matrix equation. The order of coefficient matrix used by MEI approach is much less than that used by conventional FD methods with absorbing boundary conditions, because MEI can terminate the mesh very close to the region of interested. These properties make the MEI approach a powerful tool for computational electromagnetics.

Recently, although some papers [11, 12] propose some doubts on the third postulation of the MEI coefficients, invariant to excitations, they still admit that MEI is an efficient technique to truncate mesh boundaries. Actually, their arguments did not conflict with the fundamentals of MEI, because we have already proven that MEI coefficients are actually not strictly invariant to excitations, but instead, are invariant to excitations with the error bounded by $O(h^2)$, where $h = max(h_x, h_y, h_z)$ [13]. As stated above, the general local FD equation we have developed also has the error bounded by $O(h^2)$, therefore, the total truncation/model error of the final matrix system has the order of $O(h^2)$, which is not degenerated by the introduction of MEI equations on boundaries. Up to now, MEI has been successfully used to analyze electromagnetic scattering problems and microwave integrated circuits [7, 8, 9].

However, the closed form of Green's functions for multilayer structures of VLSI interconnects, are generally derived in spectral-domain and then transformed to the space-domain by inverse Fourier transformation which are infinite integrals. In addition to the tedious deduction of Green's function in a multilayer structure, the calculation of the MEI coefficients is very time-consuming because many Sommerfeld type integrals will be encountered, which makes the calculation of MEI coefficients dominate the total computation time. As reported in [14], for a one-layer microstrip stub, obtaining the MEI coefficients required 90 CPU minutes for a single frequency, and solving the sparse system required 24 minutes. Therefore, complicated Green's function and disagreeable Sommerfeld-type integrals make MEI very difficult, if not impossible, to be applied to multilayer and multiconductor interconnects.

4 Geometry Independent Measured Equation of Invariance

In order to apply MEI to multilayer and multiconductor interconnects, we introduced the measuring box concept. A measuring box is just a closed surface that encloses all objects of interest as shown in Fig. 2 and Fig. 3, to isolate the MEI nodes from the region containing conductors. It has been demonstrated that the MEI are also independent of the source distribution on the measuring loop [10]. The MEI coefficients are then determined from the metrons on the measuring loop instead of the metrons on the conductors, which means the MEI are independent of the geometries of the conductors. The dielectric layers are truncated at the measuring loop with physical polish which ensures such truncation will not affect the total accuracy, and free space out of the measuring loop is assumed. Therefore, we can use very simple free space Green's function to measure MEI coefficients. Experiments suggest that very few layers between the measuring loop and the nearest conductors, and again very few layers outside the measuring loop are sufficient to guarantee the accuracy of results in practice. The measuring loop concept has already been successfully applied to extract 2D parasitics of multilayer multiconductor interconnects [10].

The potential values $\phi_i^k, i = 0, \ldots, M$, at each MEI node corresponding to kth metron σ^k defined on the measuring loop can be simply obtained by

$$\phi_i^k = \int_{\Gamma_e} \sigma^k(s')\, G(\vec{r}_i, \vec{r}\,')ds' \quad k = 1, \ldots, K \tag{3}$$

where Γ_e stands for the measuring loop, $\vec{r}_i, \vec{r}\,'$ denote the position vectors at ith MEI node and the measuring loop

W/H	GIMEI	Cao [4]	Hamm. [16]	Zutter [17]	Gupta [18]
0.4	92.365	92.278	90.334	90.320	90.191
0.7	73.676	73.962	72.751	72.737	72.673
1.0	62.918	62.811	61.839	61.842	61.591
2.0	42.422	42.998	42.260	42.267	42.394
4.0	26.712	26.971	26.459	26.443	26.517
10.0	12.807	12.996	12.719	12.713	12.716

Table 1: Results of the thin microstrip line

respectively, and K the number of metrons. The 3-D quasi-static Green's function of free space is simply

$$G(\vec{r}_i, \vec{r}\,') = \frac{1}{4\pi|\vec{r}_i - \vec{r}\,'|} - \frac{1}{4\pi|\vec{r}_i - \vec{r}\,''|} \tag{4}$$

where $\vec{r}\,''$ is the image position vector of $\vec{r}\,'$ with respect to the ground plane if any. Substituting the potential values ϕ_i^k produced by kth metron into MEI (Eq. 2), yields a set of linear algebraic equations with respect to the MEI coefficients $C_1, C_2, \ldots, C_M$, when C_0 is normalized to 1. In our program, the overhead time spent on MEI coefficients is only a very small part(less than 5%) in the total computing time.

Coupling the MEI equations at truncated mesh boundary nodes with the FD equations at interior nodes results in a matrix equation

$$[S]\,\bar{\phi} = \bar{f} \tag{5}$$

where $\bar{\phi}$ is a column matrix consisting of the potential values at all mesh nodes, and $\bar{f}$ the known column matrix followed from the neighboring FD's around the conductors on which voltages are impressed. From the solution of Eq. 5, we get the potential distribution over the mesh region. We use Duncan correction [15] to get charge distribution or total charge on each conductor. Bringing these charges into definition, we can get the final short circuit capacitance matrix.

5 Experimental Results

To verify the accuracy and efficiency of this method, the following examples were selected to provide a quantitative measure. The experiments were performed on a Sun Sparc 20 workstation.

Example 1. A thin microstrip line

The first example we show is microstrip line with zero thickness over a ground plane, and the dielectric constant is 6. The characteristic impedance Z_0 of this structure can be defined as $Z_0 = \frac{1}{v_0\sqrt{CC_0}}$, where v_0 is the speed of light in free space, C the capacitance of this structure, and C_0 the capacitance with dielectric layer replaced by free space. Table 1 shows the comparison of the characteristic impedance in Ohm varying with the width height ratio W/H obtained by using GIMEI, Cao's Method of Moments [4], Zutter's Space Domain Green's Function Approach(SDGA) [17], and those provided by Gupta [18] and Hammerstad [16]. In our results, we use ten mesh points

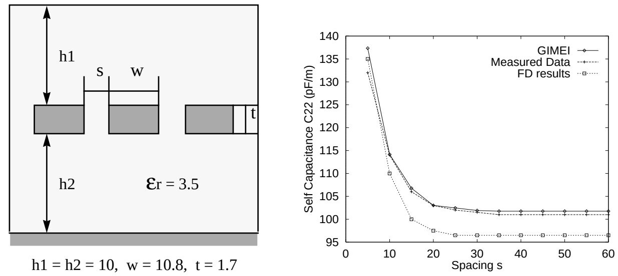

(a) configuration (b) results

Figure 4: Three parallel lines example

cubes	C_G	C_F	T_G	T_F	CPU time T_F/T_G
1x1x1	73.89	73.38	0.21	0.7	3.3
1x1x3	114.8	115	0.29	1.9	6.6
1x1x5	149.8	149.6	0.34	3.6	10.6
1x1x8	196.4	196.2	0.45	4.7	10.4
1x1x10	225.4	225	0.52	6.8	13.1

Table 2: C(pF) of the cube and CPU time(sec.)

per unit length. The difference of our results are within 2.5% compared with the results by Hammerstad [16] which is regarded as standard reference for this kind of problem.

Example 2. Three parallel lines

The second 2D example is three identical parallel wires immersed in a dielectric shown in Fig. 4(a). Fig. 4(b) shows self capacitance of the middle conductor $C22$ varying with the interwire distance. A difference of less than 3% is observed in the whole range between our results and the measured data [19]. It's clear from the figure that our results are closer to the measured data than those obtained by standard Finite Difference method(FD).

As stated in [10], GIMEI outperforms all methods for fairly large structures such as tens even hundreds of conductors on tens of dielectric layers.

For the rest of this paper, we use C_G, T_G, and M_G to denote the capacitance, CPU time, and memory usage for GIMEI, and C_F, T_F, and M_F for FASTCAP.

Example 3. A simple cube with different longitude

This is a simple example of $1 \times 1 \times z$ cube(unit is meter for simplicity) is computed and compared with FASTCAP [1]. Table 2 shows the capacitance of the cube varying with the extended edge z by GIMEI compared with those of FASTCAP as well as the CPU time of the two methods. From the table, one can clearly see that, GIMEI is generally ten times faster than FASTCAP with the difference of less than 1%.

We have also compared our results with those of standard FD with zero E field (electric wall, E.W.) boundary condition with the same mesh discretization as our method. The structure is $1 \times 1 \times 5$ cube. For our method, the buffers used outside the measuring loop is three mesh layers, the results is 149.8pF with 0.34 seconds CPU time. Table 3 shows the results by using E.W. varying with the number of layers outside the measuring loop. It can be

buffer #	C (pF)	CPU time(sec.)	matrix order
3	241.6	0.25	1,000
5	197	1.89	5,000
10	174	9.1	20,000
15	164	28.67	50,000
20	159.4	68.45	100,000
25	155	146.76	200,000
30	151	250.58	300,000

Table 3: Results of $1 \times 1 \times 5$ meters cube using E.W. boundary condition

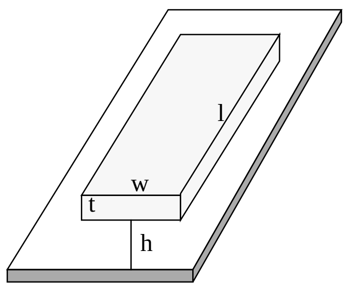

Figure 5: Single plate on ground plane

structure	C_G	[20]	C_F	T_G	T_F
$t = 0.5\mu$ $h = 0.8\mu$	3.87	4.00	2.34	0.49	4.61
$t = 1.0\mu$ $h = 2.0\mu$	2.408	2.47	2.21	0.39	1.26

Table 4: Comparison of capacitance in fF and CPU time in sec.

seen that, to achieve the similar accuracy, standard FD with E.W. boundary condition needs more than 30 mesh layers and consumes much more CPU time and memory than GIMEI.

Example 4. Single plate over a ground plane

Fig.5 is a single plate with finite length put over a ground plane. The structure parameters are $l = 10\mu, w = 5\mu, \varepsilon_r = 3.9$. Table 4 shows the results of out method, FASTCAP, and those in [20], which is a closed form formula with 10% error. It is clear that for the smaller geometry, FASTCAP did not give the right answer.

Example 5. A bend with numerical experimental on proper selection of buffer number

A simple right-angel bend is shown in Fig.6, where all dimensions are in meters. This configuration is actually got from [3]. Using GIMEI, the results(self capacitance of the bend) is $2.974nF$ with $1.16sec.$ CPU time, while FASTCAP got $2.956nF$ with $16.1sec.$ CPU time. GIMEI is more than ten times faster than FASTCAP. It should be noticed that in the original paper[3], the result is $105F$ which is unreasonable. Fig.6(b) shows the capacitance obtained by GIMEI varying with the buffer number, which is

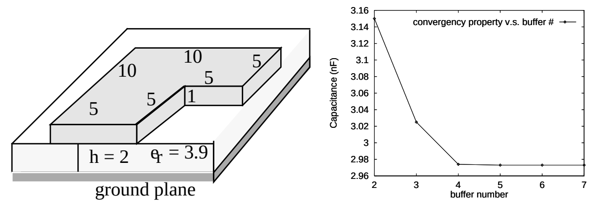

(a) Configuration (b) C vs buffer number

Figure 6: The bend problem

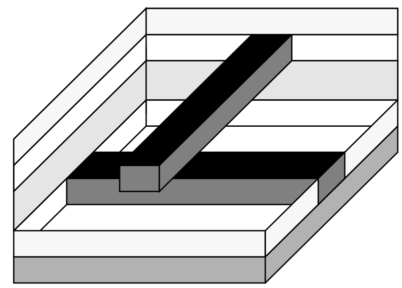

Figure 7: A 1×1 cross over on ground plane

z	C_{11G}	C_{11F}	C_{22G}	C_{22F}	C_{12G}	C_{12F}
4	230	226	180.6	176	-61	-60.41
5	260	265	203.5	205	-66.5	-68.43
7	348.7	341.4	260.1	253.7	-80.1	-79
10	440.3	451.6	326.8	324.2	-86	-87

Table 5: Capacitance in pF for $1 \times 1 \times z$ cross over problem

the number of layers used outside the measuring loop. As stated above, we only need to use four to five buffer layers to get accurate results.

Example 6. A series of 1×1 crossover

Fig.7 shows a 1×1 crossover immersed in five layer dielectric with a ground plane at the very bottom of the structure. The structure parameters are: the height of each dielectric layer is 1, each metal line has the width of 1, and the two lines have the same length z. They are overlapped both in the middle of the other line. The dielectric relative permittivities are all chosen to be 3.9 for the case of simplicity. The lower metal is numbered 1 while the higher numbered 2.

Table 5 shows the results of capacitances C_{11}, C_{22} and C_{12} computed by GIMEI and FASTCAP varying with the

z	T_G	T_F	CPU time T_F/T_G	M_G	M_F	Memory M_F/M_G
4	2.8	24.4	8.7	3.5	22	6.3
5	3.2	26.0	8.1	3.7	25	6.6
7	6.5	65.6	10.1	5.6	60	10.7
10	9.2	93.2	10.2	6.5	78	12

Table 6: Comparison of CPU time in sec. and memory in MB for crossover problem

line length z. Here, the number of buffer layer outside the measuring loop is chosen to be 3. The two results are within the difference of 3%. Table 6 shows the CPU time and memory use of the two methods. It's clear that GIMEI is around ten times faster that FASTCAP and consumes much less memory.

6 Conclusions

In this paper, by using the measuring box concept, we substantially improved the MEI in three key aspects: 1) cancelled the postulate of geometry specific in conventional MEI, 2) avoided the deduction of Green's function in multilayer structure, and 3) avoided the calculation of disagreeable Sommerfeld type integrals, but still keep all the advantages of MEI, and successfully introduce the concept of MEI as an efficient truncation boundary condition into the analysis of three-dimension interconnects. Using GIMEI, the calculation of MEI coefficients only costs a very little part of the total computing time. Experimental results show that the geometry independent MEI proposed in this paper is generally an order of magnitude faster than FASTCAP using BEM with multipole acceleration without loss of accuracy. GIMEI can generally treat larger structures faster than other numerical methods. Furthermore, this technique can easily handle the interconnect problems with arbitrarily-shaped cross section and lossy and inhomogeneous dielectric media due to the nature of Finite Difference used inside the measuring box. The technique are also being extended to 2-D or 3-D dynamic analysis of multilayer multiconductor interconnect parasitic (including both capacitance and inductance) extraction.

References

[1] K. Nabors and J. White, "Multipole-accelerated capacitance extraction algorithms for 3-D structures with multiple dielectrics," *IEEE Trans. on CAS I: Fundamental Theory and App.*, vol. 39, pp. 946–954, November 1992.

[2] G. Costache, "Finite element method applied to skin-effect problems in strip transmission lines," *IEEE Tran. on MTT*, vol. MTT-35, pp. 1009–1013, November 1987.

[3] A. Zemainian and R. Tewarson, "Three dimensional capacitance computations for VLSI/ULSI interconnections," *IEEE Tran. on CAD*, vol. CAD-8, pp. 1319–1326, December 1989.

[4] W. Cao, R. Harrington, J. Mantz, and T. Sarkar, "Multiconductor transmission lines in multilayered dielectric media," *IEEE Tran. on MTT*, vol. MTT-32, pp. 439–450, April 1984.

[5] G. Pan, G. Wang, and B. Gilbert, "Edge effect enforced boundary element analysis of multilayered transmission lines," *IEEE Tran. on CAS I: Fundamental Theory and App.*, vol. 39, pp. 955–963, November 1992.

[6] K. Mei, R. Pous, Z. Chen, and Y. Liu, "The measured equation of invariance: A new concept in field computation," in *IEEE AP-S, Digest*, pp. 2047–2050, July 1992.

[7] Y. Li, Z. J. Cendes, and X. Yuan, "A modified mei method for solving scattering problems with the finite element method," in *IEEE AP-S, Digest*, pp. 284–287, July 1993.

[8] W. Hong, Y. Liu, and K. Mei, "Application of the measured equation of invariance to solve scattering problems invovling penetrable medium," *Radio Science*, April 1994.

[9] W. Hong and K. Mei, "Application of the measured equation of invariance to the scattering problem of an anisotropic medium cylinder," in *IEEE AP-S, Seattle*, June 1994.

[10] W. Hong, W. Sun, and W. Dai, "Fast parameters extraction of multilayer multiconductor interconnects using geometry independent measured equation of invariance," in *proceedings of IEEE MCM Conference*, February 1996.

[11] J. O. Jevtic and R. Lee, "A theoretical and numerical analysis of the measured equation invariance," *IEEE Trans. on AP*, pp. 1097–1105, August 1994.

[12] J. O. Jevtic and R. Lee, "How invariance is the measured equation invariance," *IEEE Microwave and Guided Wave Letters*, pp. 45–47, February 1995.

[13] W. Hong, W. Sun, and W. Dai, "On the invariance of measured equation of invariance," Tech. Rep. UCSC-CRL-95-45, UCSC, Santa Cruz, 1995.

[14] M. D. Prouty, *Application of the Mesuared Equation of Invariance to Planar Microstrip Structures.* PhD thesis, University of California at Berkeley, 1994.

[15] J. Duncan, "The accuracy of finite difference solutions of Laplace's equation," *IEEE Trans. on MTT*, pp. 575–582, 1967.

[16] E. Hammerstad and O. Jensen, "Accurated models for microstrip computer-aided design," in *IEEE MTT-S, Digest*, pp. 407–409, 1980.

[17] W. Delbare and D. Zutter, "Space-domain green's function approach to the capacitance calculation of multiconductor lines in multilayered dielectrics with improved surface charge modeling," *IEEE Trans. on MTT*, pp. 1562–1568, Octomber 1989.

[18] K. Gupta, R. Gary, and I. J. Bahl, *Microstrip Lines and Slotlines.* Artch House, 1979.

[19] M. Lin, "Measured capacitance coefficients of multiconductor microstrip lines with small dimensions," *IEEE Trans. on CHM*, pp. 1050–1054, December 1990.

[20] T. Sakurai and K. Tamaru, "Simple formulas for two- and three-dimensional capacitances," *IEEE Tran. on ED*, vol. ED-30, pp. 183–185, February 1983.